

Variation of Ferroptosis-Related Markers in HaCaT Cell Photoaging Models Induced by UVB

Peng-Cheng Zhang^{1,2}, Yi Hong³, Shi-Qin Zong^{1,2}, Long Chen^{1,2}, Chong Zhang⁴, Dai-Zhi Tian⁴, Dan Ke⁵, Li-Ming Tian^{1,2,4}

¹Department of Dermatology, Traditional Chinese and Western Medicine Hospital of Wuhan, Tongji Medical College, Huazhong University of Science and Technology, Wuhan, 430022, People's Republic of China; ²Hubei Provincial Key Laboratory of Skin Infection and Immunity, Wuhan No.1 Hospital, Wuhan, 430022, People's Republic of China; ³College of Pharmacy, Hubei University of Chinese Medicine, Wuhan, 430065, People's Republic of China; ⁴Institute of Geriatrics, Hubei University of Chinese Medicine, Wuhan, 430065, People's Republic of China; ⁵Department of Dermatology, Chongqing Traditional Chinese Medicine Hospital, Chongqing, 400000, People's Republic of China

Correspondence: Dan Ke, Department of Dermatology, Chongqing Traditional Chinese Medicine Hospital, No. 40 of Daomenkou, Yuzhong District, Chongqing, 400000, People's Republic of China, Tel +86 23 6390 1120, Fax +86 23 6373 1325, Email 2306896229@qq.com; Li-Ming Tian, Department of Dermatology, Traditional Chinese and Western Medicine Hospital of Wuhan, Tongji Medical College, Huazhong University of Science and Technology, No. 215 of Zhongshan Avenue, Qiaokou District, Wuhan, 430022, People's Republic of China, Tel +86 27 8533 2606, Fax +86 27 8583 2563, Email jolly0731@126.com

Objective: To investigate the variation of ferroptosis-related markers in HaCaT cell photoaging models induced by ultraviolet-B (UVB).

Methods: UVB-treated HaCaT cells served as the model (UVB group) for cellular photoaging, whereas untreated HaCaT cells served as the control group. HaCaT cells were exposed to UVB and the ferroptosis inhibitor Ferrostatin-1 (Fer-1) as part of the UVB+Fer-1 group, and co-cultured with the ferroptosis inducer Erastin as part of the UVB+Erastin group. Reactive oxygen species (ROS) detection kit and senescence-related β galactosidase (SA- β -gal) staining were used to evaluate the senescence of HaCaT cells. Lipid reactive oxygen species were detected by C11 BODIPY581/591 probe and mitochondrial morphology was observed by transmission electron microscopy. The mRNA expressions of glutathione peroxidase 4 (GPX4) and ferroptosis-suppressor-protein 1 (FSP1) were detected by real-time reverse transcription-PCR (RT-RCP), and the level of GPX4 protein was measured by immunofluorescence assay.

Results: The UVB group had considerably greater levels of ROS, SA- β -gal, and lipid reactive oxygen species than the control group. The UVB group's mitochondrial volume was reduced, the membrane density increased, and the mitochondrial crest decreased or even disappeared. GPX4 and FSP1 expression levels were similarly found to be lower in the UVB group. Furthermore, the positive rate of SA- β -gal and lipid reactive oxygen species in the UVB+Fer-1 group was much lower than in the UVB group, but it was reverse in the UVB+Erastin group. This study showed that induced ferroptosis can aggravate aging, and vice versa.

Conclusion: According to the findings, ferroptosis may be linked to UVB-induced skin photoaging, which could be attenuated by inhibition of ferroptosis.

Keywords: skin aging, ferroptosis, oxidative stress

Introduction

Photoaging skin is characterized by rough skin surface, reduced water content and elasticity, and even abnormal pigmentation, which has a major impact on patients' physical appearance and mental health.^{1,2} For example, common clinical diseases such as chloasma are the manifestations of skin photoaging. However, there are few effective and significant drugs for the treatment of the above diseases.^{3,4} Studies have revealed that prolonged exposure of skin to UVB radiation is the principal cause of photoaging.⁵ Excessive exposure to UVB radiation is a trigger for excessive production of ROS, and one of the main reasons for accelerating skin photoaging.^{6,7} UVB can induce epidermal cells to create a substantial amount of ROS, cause oxidative damage to intracellular molecules, and activate a series of signaling pathways that accelerate skin aging.^{6,7}

Ferroptosis is a type of controlled cell death that is characterized by an excessive buildup of lipid ROS induced by an excess of intracellular free divalent iron. Ferroptosis plays an important role in the aging and development of different

species, and it may be involved in the aging of many organs.⁸ Ferroptosis has been linked to age-related disorders such as diabetes, malignancies, hypertension, and neurological diseases.^{8,9} Typical cell morphological alterations associated with ferroptosis include diminished or absent cristae, enhanced bilayer membrane density, and mitochondrial atrophy.¹⁰ Fer-1, a lipophilic molecule, has been shown to reduce ferroptosis by preventing the buildup of lipid reactive oxygen species, whereas Erastin, a ferroptosis inducer, has been shown to enhance ferroptosis.¹¹

Some scholars have analyzed the FerrDb database and found that exposure to cigarette smoke will cause the ferroptosis of female skin, which will then aggravate the female skin aging.¹² However, studies on ferroptosis and skin aging have rarely been reported. In particular, studies of ferroptosis and skin photoaging have not been specifically described.

To further verify, we established a photoaging model of HaCaT cells triggered by UVB, and observed changes in lipid reactive oxygen species, mitochondrial morphology, and the expression of proteins linked to ferroptosis (GPX4 and FSP1). At the same time, we treated the cells with Fer-1 and Erastin, and observed the changes of SA- β -gal and lipid ROS in HaCaT cells. Finally, we found that ferroptosis may be a potential mechanism leading to skin photoaging, which may provide new ideas for the future development of medicinal targets to fight the effects of skin photoaging.

Materials and Methods

Materials and Reagents

HaCaT cells, trypsin (Gibco, USA) and penicillin-streptomycin (PM150210, Gibco, USA) were bought from Procell Life Science&Technology Co.,Ltd. (Wuhan, China). Fer-1 and Erastin were purchased from MedChemexpress (USA). SA- β -gal staining kits and ROS test kit were purchased from Beyotime Biotechnology Co., Ltd. (Shanghai, China). DCFH-DA probe was purchased from Solebo Technology Co., Ltd. (Beijing China). C11 BODIPY 581/591 probe was purchased from Invitrogen (USA). Ultracut slicer and laser confocal microscope were purchased from Leica (Germany). Transmission electron microscope was purchased from Hitachi (Japan). PCR primers were synthesized by bioengineering Co., Ltd. (Shanghai, China). Trizol lysis buffer was purchased from Takara (USA).

Cell Culture

The cells were grown in DMEM media containing ten percent fetal bovine serum and a single percent penicillin-streptomycin.

HaCaT Cell Photoaging Model and Grouping

In DMEM high glucose media with 10% fetal bovine serum, HaCaT cells were grown. To cause photoaging, the cells were exposed to UVB radiation three times, once every other day. The emission wavelength of the ultraviolet lamp is 311 nm, and the single irradiation dose is 20 mJ. The HaCaT cells were divided into the following groups: normal, UVB, UVB+Fer-1 (1 μ M), and UVB+Erastin (5 μ M).

SA- β -Gal Staining

SA- β -gal staining kits were used to colorize HaCaT cells. After 72 hours of the last irradiation, the cell culture media was taken out and cleaned with PBS. The 1mL fixing solution was added and fixed at room temperature for 15 minutes. Following that, samples were washed three times in PBS for 3 minutes each time. After the moisture was removed, 1mL staining solution was added to each well and placed in a wet box at 37 °C overnight. The morphology and staining of cells were observed under an optical microscope.

ROS Detection

A ROS test kit was used to assess intracellular ROS levels. Following treatment, HaCaT cells were incubated in the dark for 30 minutes with the DCFH-DA probe at 37°C. The cells were then digested with trypsin after being rinsed with PBS. Cells were collected after centrifugation at 1100 \times g for 3 minutes. The cells were resuspended in PBS after the supernatant

was discarded. Flow cytometry was used to measure the fluorescence intensity in line with the manufacturer's requirements.

Lipid ROS Detection

A C11 BODIPY 581/591 probe was used to measure lipid ROS. The 1 mg BODIPY 581/591 sample was dissolved in 198.2554 μ L DMSO to prepare a 10 mM storage solution. The cells were then treated with the probe for an hour before being rinsed three times. The fluorescence signal images under 505–550 nm and > 580 nm were detected and collected. Image J software was used to do a semi-quantitative study of fluorescence intensity.

Transmission Electron Microscope

After digestion and centrifugation, the cells were fixed with 2% glutaraldehyde. Then, the cells were fixed with 1% osmic acid again. The specimens were dehydrated, infiltrated and embedded in the LX-112 embedding solution, and polymerized in an oven at 60 °C for about 3 days. The sections were sliced in a Ultracut slicer and processed with lead citrate and uranyl acetate. For image capture, a transmission electron microscope (HT7800) was employed.

RT-PCR

Total RNA was extracted with Trizol lysis buffer, and was then transformed into cDNA. PCR primers were synthesized by bioengineering Co., Ltd. (Shanghai, China). GPX4 forward primer 5'-CCT GGA CAA GTA CCG GGG CT-3', reverse primer 5'-AAA CCA CAC TCA GCG TAT CG-3'; FSP1 forward primer 5'-ACA TGG TGA GGC AGG TCC A-3', reverse primer 5'-GCC ACT TGG GAG TGA ATG AG -3'; GADPH forward primer 5'-GAA GGT GAA GGT CGG AGT C-3', reverse primer 5'-GAA GAT GGT GAT GGG ATT TC-3'. Target gene PCR reactions were quantitated using TOYOBO's QPK-201 SYBR Green real-time reverse transcription-PCR Master Mix. PCR reaction system (20 μ L): SYBR Premix 5 μ L, cDNA template 2 μ L, forward and reverse primers 0.5 μ L each, double distilled water 7.2 μ L. PCR reaction conditions: 96 °C 1 min, 95 °C 15s, 60 °C 1 min, 95 °C 15s, total 40 cycles. Using the internal reference gene GADPH, the $2^{-\Delta\Delta Ct}$ technique was used to determine the target gene's relative expression.

GPX4 Expression Was Detected by Immunofluorescence

The digested cells were resuspended and centrifuged before being injected into 24-well plates. After being fixed for 10 to 15 minutes, the cells were permeated with 0.2% Triton X-100 and repeatedly rinsed. After covering the slides with ten percent goat serum for a thirty-minute period, the primary antibody was allowed to incubate overnight before being followed by a 1-hour secondary antibody incubation. The cells were then rinsed one more three to five times in the dark after the secondary antibody solution was removed. Using a laser confocal microscope, images were acquired after staining.

Statistical Analysis

The data were examined using SPSS 23.0 statistical software. Each group's quantitative results were represented as $\bar{X} \pm s$. One-way ANOVA test was used for comparisons between multiple groups, and independent sample *t*-test for comparison between two groups. Statistics were deemed significant at $P < 0.05$. The program "GraphPad Prism 5" was used to analyze and draw all histograms in this article.

Results

Effects of UVB Irradiation on ROS and SA- β -Gal in HaCaT Cells

Using flow cytometry, the intracellular ROS content was determined. Figure 1a illustrates that the UVB group's ROS content was substantially greater than the normal group's. It was observed that HaCaT cells in UVB group became round, shrunken, with unclear outline and disordered arrangement. The SA- β -gal staining revealed more positive cells, which corresponded to the morphological characteristics of senescent cells. According to statistics, the positive rate of SA- β -gal in the UVB group was statistically substantially greater than that in the normal group (Figure 1b). These results indicated that HaCaT cells in UVB group showed obvious senescence.

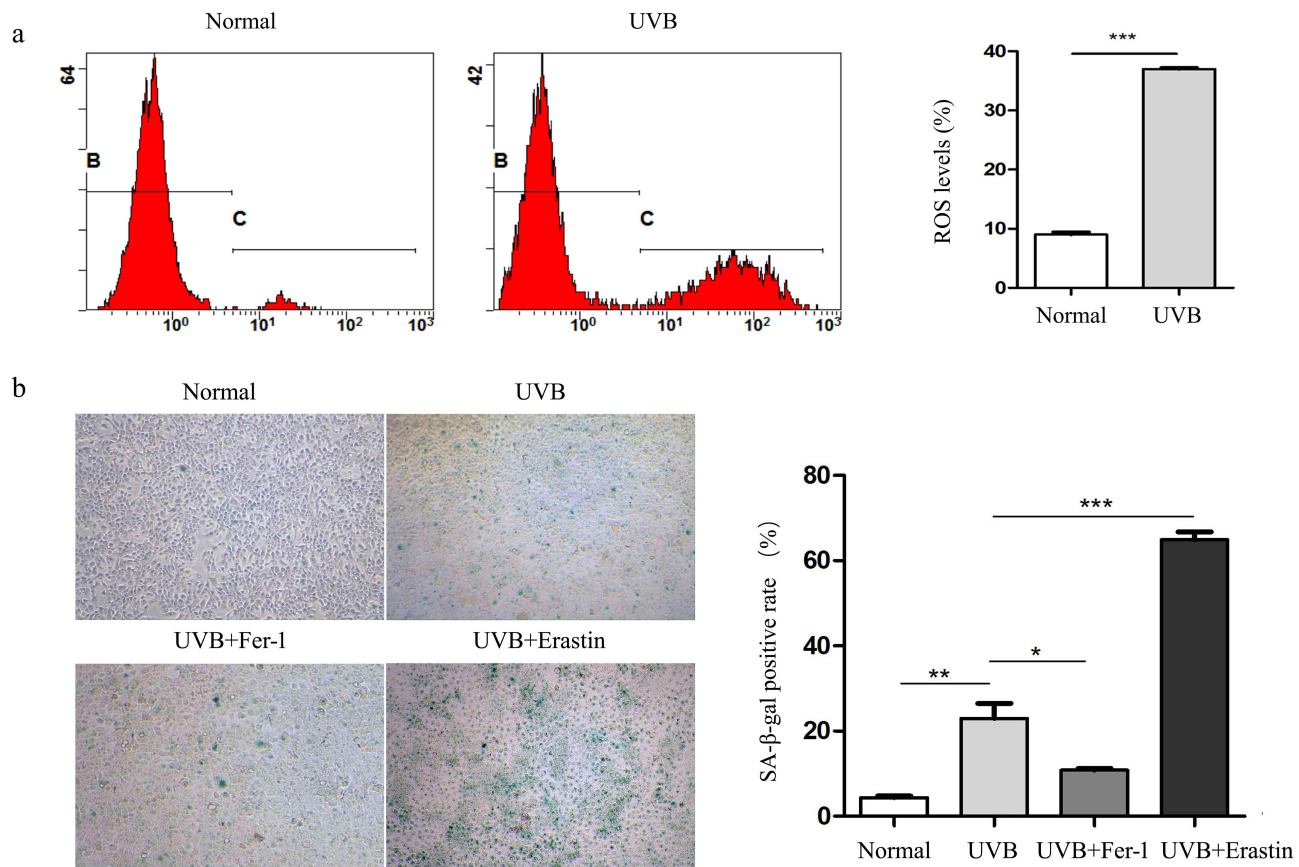


Figure 1 UVB irradiation induced HaCaT cell senescence. (a) Flow cytometry (FITC-A) was used to measure the amount of ROS in HaCaT cells. (b) The morphology and SA-β-gal activity of HaCaT cells stained with SA-β-gal staining kits were observed under microscope ($\times 100$). * $P < 0.05$; ** $P < 0.01$; *** $P < 0.001$.

Effects of UVB Irradiation on Lipid ROS and Mitochondrial Morphology in HaCaT Cells

Next, we further examined the changes of ferroptosis-related indicators in HaCaT cells. Using the C11 BODIPY 581/591 probe, HaCaT cells were labeled for laser confocal scanning microscopy analysis. The results showed that the lipid ROS in UVB group HaCaT cells was obviously greater than that in the normal group (Figure 2). Moreover, it was observed by transmission electron microscope that the mitochondrial volume was smaller, the membrane density increased, and the mitochondrial cristae decreased or even disappeared, which was in accordance with the characteristics of ferroptosis (Figure 3).

UVB Irradiation Down-Regulated the Levels of GPX4 and FSP1 in HaCaT Cells

GPX4 and FSP1 mRNA levels in HaCaT cells in the UVB group were undoubtedly reduced than those in the normal group, according to the results of RT-PCR (Figure 4). The results of immunofluorescence semi-quantitative showed that GPX4 protein was markedly down-regulated in HaCaT cells of UVB group, as shown in Figure 5.

Ferroptosis Inhibition or Induction Can Affect the Morphology, Positive Rate of SA-β-Gal Staining and Lipid ROS Generation in HaCaT Cells

The results of the detection of the markers related to ferroptosis mentioned above suggested that more severe iron death may have occurred in photoaging HaCaT cells. Therefore, we pretreated some HaCaT cells with ferroptosis inhibitor Fer-1 ($1\mu\text{M}$) and inducer Erastin ($5\mu\text{M}$) to observe cell morphology and test the activity of SA-β-gal and the content of lipid reactive oxygen species. Compared with UVB group, the morphology of HaCaT cells in UVB+Fer-1 group was more consistent and the outline

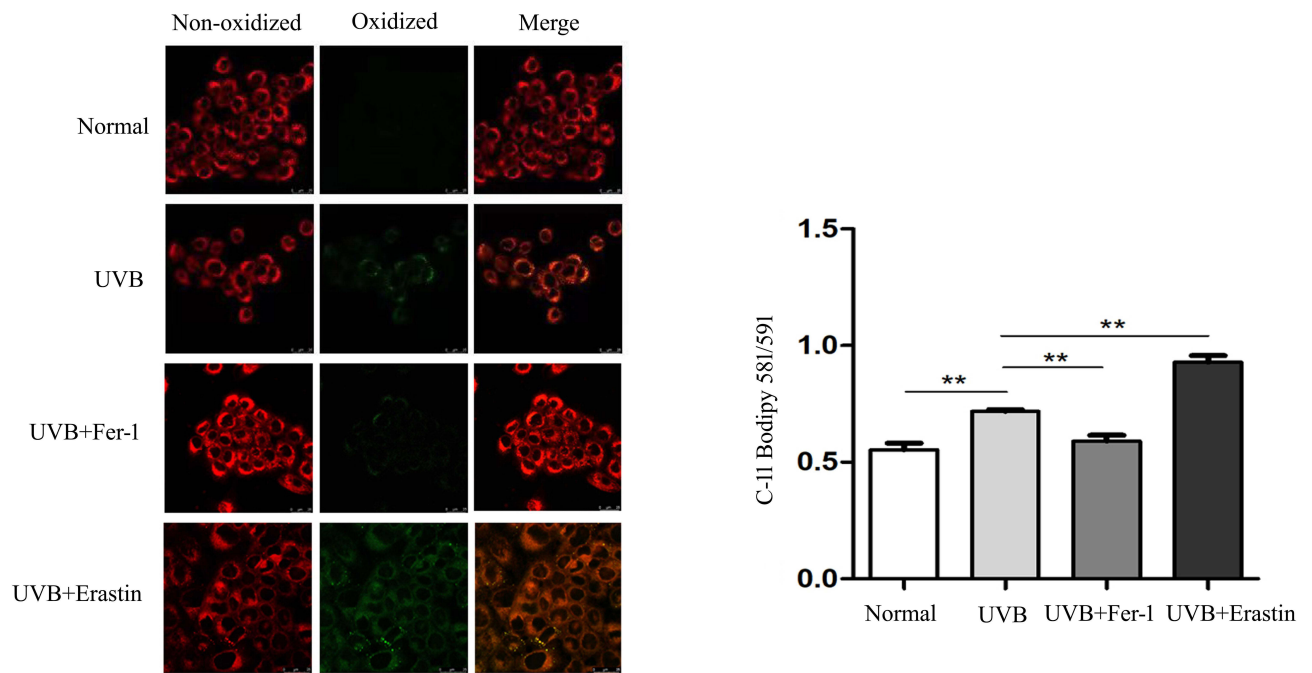


Figure 2 Lipid ROS were identified in each group using the CII BODIPY 581/591/probe (×400). **P<0.01.

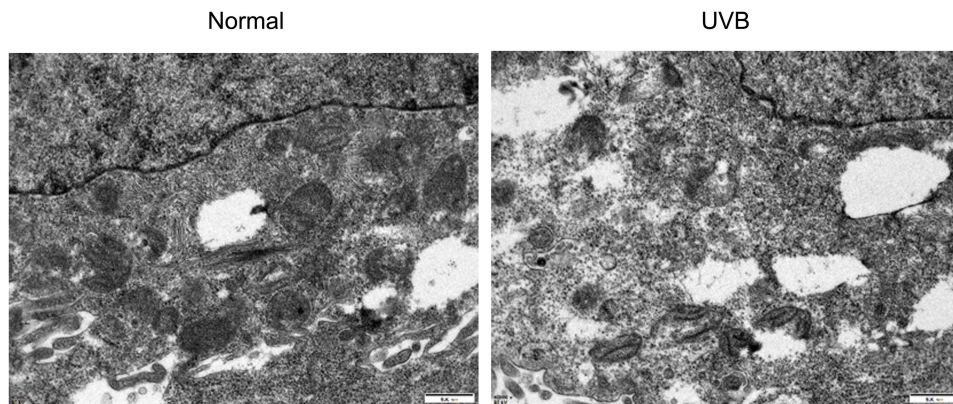


Figure 3 The mitochondrial morphology of HaCaT in two groups was detected by transmission electron microscope (×10.0K).

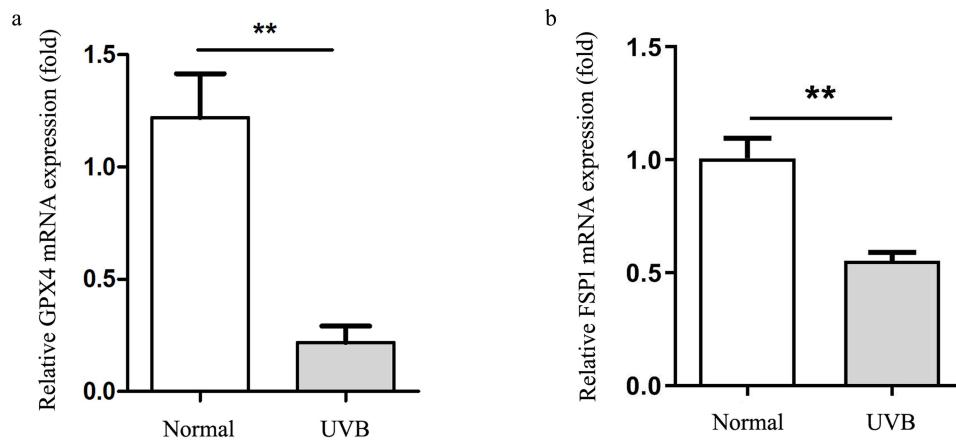


Figure 4 The expression of GPX4 (a) and FSP1 (b) mRNA in HaCaT cells was measured using RT-PCR. **P<0.01.

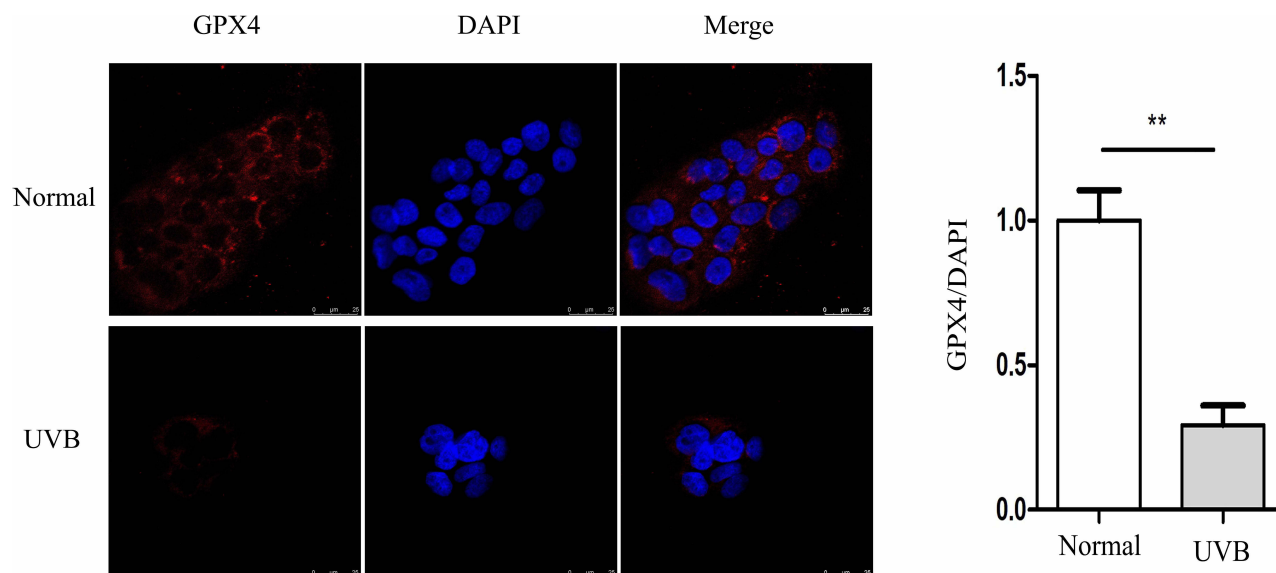


Figure 5 The level of GPX4 protein was detected by immunofluorescence ($\times 400$). $**P < 0.01$.

was still discernible under light microscope. The positive rate of SA- β -gal was much lower in the UVB + Fer-1 group than in the UVB group. On the contrary, the outline of HaCaT cells in UVB+Erastin group was blurred and the arrangement was more disordered, and the positive rate of SA- β -gal was significantly higher (Figure 1b). In addition, the amount of lipid ROS in HaCaT cells decreased significantly after treatment with Fer-1, while that in UVB + Erastin group increased (Figure 2).

Discussion

One of the most obvious signs of aging is skin aging, which is controlled by a number of endogenous and external variables.⁷ Ultraviolet radiation is the main environmental factor that accelerates skin aging, which is called skin photoaging.¹³ The mechanism of UV-induced photoaging is very complex and not yet fully understood, but it is intimately connected to skin cell damage caused by oxidative stress and inflammation.^{14–16}

Ferroptosis is a kind of cell death that differs from apoptosis in that it is driven by iron-dependent lipid reactive oxygen species.⁸ It is not difficult to see that the primary cause of ferroptosis is an overabundance of lipid ROS, which is brought on by an imbalance between the lipid oxidation and antioxidant system. Excessive lipid ROS cause damage to a number of crucial functional compounds within cells, a process that is similar to that of UVB-induced oxidative stress injury and skin photoaging.^{8,14} Therefore, does UVB-induced skin photoaging also entail ferroptosis? First, we conducted a study of the pertinent literature and discovered that ferroptosis may mediate oxidative stress and inflammation,^{17,18} and is crucial for the healthy lifespan of nematodes, human degenerative diseases, and inflammatory skin disorders.^{8,19,20} Specifically, the ferrous iron in nematodes increase with age, which induces ferroptosis by producing a large amount of ROS to shorten the lifespan. And L-threonine supplementation can reduce ferroptosis in a ferritin-dependent manner to increase the healthy lifespan of nematodes.¹⁹ In humans, iron homeostasis and ferroptosis have been associated to the etiology of Alzheimer's disease. For instance, the brain tissue of Alzheimer's patients exhibits the characteristics of ferroptosis, such as iron buildup and lipid ROS accumulation.²¹ In addition, researchers have observed abnormal lipid expression and metabolism correlated with ferroptosis in keratinocytes in psoriatic lesions.²² UVB irradiation on epidermal keratinocytes can activate ferroptosis, apoptosis, pyroptosis, et al, and ferroptosis is closely related to UVB-induced skin inflammation.²³ Skin inflammation is also a promoter of skin aging.²⁴ According to the literature mentioned above, UVB irradiation may cause ferroptosis, and ferroptosis may further exacerbate skin photoaging. However, there are yet no concrete instances of ferroptosis-related skin photoaging.

Therefore, in order to further verify the speculation, we used UVB to induce photoaging of HaCaT cells. As everyone knows that UVB radiation leads to skin photoaging mainly through the generation of ROS.²⁵ Skin photoaging due to acute and chronic exposure to UVB irradiation causes characteristic molecular changes including ROS formation.²⁶ The senescence-associated β -galactosidase (SA- β -gal), which is a biomarker of skin aging.²⁷ The findings of our study, ROS and SA- β -gal showed significant changes in HaCaT intracellular by UVB irradiation. The changes of these important indicators indicate successful induction of skin photoaging model. And we detected the changes of lipid reactive oxygen species, mitochondrial morphology and related molecules (GPX4 and FSP1), which had an equivalent regulatory function during ferroptosis. The primary regulator of ferroptosis, GPX4, is in charge of changing harmful lipid hydroperoxides into benign phosphatidyl alcohols in order to prevent ferroptosis.²⁸ FSP1 can inhibit ferroptosis by capturing lipid peroxide radicals through coenzyme Q10.²⁹ It is not difficult to see that the above molecules belong to the system of resistance to ferroptosis. When the molecules that inhibit ferroptosis decrease and / or the substances that promote ferroptosis increase, ferroptosis will be aggravated. Consistent with expectations, the production of GPX4 and FSP1 in HaCaT cells in UVB group was dramatically down-regulated, whereas the number of lipid ROS was significantly increased. Mitochondria also showed typical morphological changes of ferroptosis, accompanied by increased intracellular oxidative stress and increased SA- β -gal. Following that, we utilized Erastin and Fer-1 to stimulate and inhibit ferroptosis, respectively, and examined the morphology of HaCaT cells, the positive rate of SA- β -gal staining and the changes in lipid ROS. According to the findings, promoting ferroptosis might increase SA- β -gal concentration and lipid ROS expression in HaCaT cells, which further accelerated skin photoaging. In contrast, preventing ferroptosis can lessen the buildup of SA- β -gal and lipid ROS in HaCaT cells, thereby alleviating skin photoaging.

Limitations

First, a single HaCaT skin photoaging model is relatively limited. More models of skin photoaging are needed to argue our view, such as normal human skin epidermal cell lines or normal human skin tissues should be used for the model. Second, This paper is only a preliminary study on ferroptosis and skin aging. We will do more work on the molecular mechanism of ferroptosis leading to skin aging in the future.

Conclusion

In summary, this study showed that in photoaged HaCaT cells, the indicators of promoting ferroptosis were significantly up-regulated, the markers of inhibition of ferroptosis were down-regulated, and the mitochondria also showed the characteristics of ferroptosis. Moreover, induced ferroptosis can aggravate aging, and vice versa. This suggests that ferroptosis may act as a promoter of skin photoaging, and that inhibiting ferroptosis may be an effective way to prevent premature aging of the skin in the future. Nevertheless, the specific mechanism of ferroptosis affecting skin photoaging remains to be further studied.

Author Contributions

All authors made a corresponding contribution to the work reported, whether that is in the conception, study design, execution, acquisition of data, analysis and interpretation, or in all these areas; took part in drafting, revising or critically reviewing the article; gave final approval of the version to be published; have agreed on the journal to which the article has been submitted; and agree to be accountable for all aspects of the work.

Funding

National Natural Science Foundation of China (81674039, 81873347); Key Projects of Scientific Research Fund of Traditional Chinese Medicine of Hubei Health Commission (ZY2021Z011); Training Project Funding Plan of Young-aged Talent of Health System in Hubei Province (2020–2023); Key Projects of Chongqing Municipal Health Commission and Science and Technology Bureau Joint Medical Research (2022ZDXM037); Key Projects of Traditional Chinese Medicine of Wuhan Municipal Health Commission (WZ22A03).

Disclosure

The authors report no conflicts of interest in this work.

References

- Choi SI, Han HS, Kim JM, et al. Eisenia bicyclis extract repairs UVB-induced skin photoaging in vitro and in vivo: photoprotective effects. *Mar Drugs*. 2021;19(12):693. doi:10.3390/md19120693
- Favas R, Morone J, Martins R, et al. Cyanobacteria secondary metabolites as biotechnological ingredients in natural anti-aging cosmetics: potential to overcome hyperpigmentation, loss of skin density and UV radiation-deleterious effects. *Mar Drugs*. 2022;20(3):183. doi:10.3390/md20030183
- Lakhdar H, Zouhair K, Khadir K, et al. Evaluation of the effectiveness of a broad-spectrum sunscreen in the prevention of chloasma in pregnant women. *J Eur Acad Dermatol Venereol*. 2007;21(6):738–742. doi:10.1111/j.1468-3083.2007.02185.x
- McKesej J, Tovar-Garza A, Pandya AG. Melasma treatment: an evidence-based review. *Am J Clin Dermatol*. 2020;21(2):173–225. doi:10.1007/s40257-019-00488-w
- Sachs DL, Varani J, Chubb H, et al. Atrophic and hypertrophic photoaging: clinical, histologic, and molecular features of 2 distinct phenotypes of photoaged skin. *J Am Acad Dermatol*. 2019;81(2):480–488. doi:10.1016/j.jaad.2019.03.081
- Kammeyer A, Luiten RM. Oxidation events and skin aging. *Ageing Res Rev*. 2015;21:16–29. doi:10.1016/j.arr.2015.01.001
- Woodby B, Penta K, Pecorelli A, et al. Skin health from the inside out. *Annu Rev Food Sci Technol*. 2020;11:235–254. doi:10.1146/annurev-food-032519-051722
- Stockwell BR. Ferroptosis turns 10: emerging mechanisms, physiological functions, and therapeutic applications. *Cell*. 2022;185(14):2401–2421. doi:10.1016/j.cell.2022.06.003
- Zhou RP, Chen Y, Wei X, et al. Novel insights into ferroptosis: implications for age-related diseases. *Theranostics*. 2020;10(26):11976–11997. doi:10.7150/thno.50663
- Chen X, Kang R, Kroemer G, et al. Organelle-specific regulation of ferroptosis. *Cell Death Differ*. 2021;28(10):2843–2856. doi:10.1038/s41418-021-00859-z
- Jiang X, Stockwell BR, Conrad M. Ferroptosis: mechanisms, biology and role in disease. *Nat Rev Mol Cell Biol*. 2021;22(4):266–282. doi:10.1038/s41580-020-00324-8
- Zhang Q, Tang S, Huang G, et al. Cigarettes, a skin killer! Cigarette smoke may cause ferroptosis in female skin. *J Cosmet Dermatol*. 2022;21(7):3085–3094. doi:10.1111/jocd.14559
- Foster AR, El Chami C, O'Neill CA, et al. Osmolyte transporter expression is reduced in photoaged human skin: implications for skin hydration in aging. *Ageing Cell*. 2020;19(1):e13058. doi:10.1111/ace1.13058
- Papaccio F, D Arino A, Caputo S, et al. Focus on the contribution of oxidative stress in skin aging. *Antioxidants*. 2022;11(6):1121. doi:10.3390/antiox11061121
- Li N, Liu T, Zhu S, et al. Corylin from *Psoralea fructus* (*Psoralea corylifolia* L.) protects against UV-induced skin aging by activating Nrf2 defense mechanisms. *Phytother Res*. 2022;36(8):3276–3294. doi:10.1002/ptr.7501
- Bosset S, Bonnet-Duquenois M, Barré P, et al. Photoageing shows histological features of chronic skin inflammation without clinical and molecular abnormalities. *Br J Dermatol*. 2003;149(4):826–835. doi:10.1046/j.1365-2133.2003.05456.x
- Zhao S, Huang M, Yan L, et al. Exosomes derived from baicalin-pretreated mesenchymal stem cells alleviate hepatocyte ferroptosis after acute liver injury via the Keap1-NRF2 pathway. *Oxid Med Cell Longev*. 2022;2022:8287227. doi:10.1155/2022/8287227
- Liu N, Liang Y, Wei T, et al. The role of ferroptosis mediated by NRF2/ERK-regulated ferritinophagy in CdTe QDs-induced inflammation in macrophage. *J Hazard Mater*. 2022;436:129043. doi:10.1016/j.jhazmat.2022.129043
- Kim J, Jo Y, Cho D, et al. L-threonine promotes healthspan by expediting ferritin-dependent ferroptosis inhibition in *C. elegans*. *Nat Commun*. 2022;13(1):6554. doi:10.1038/s41467-022-34265-x
- Angelova PR, Esteras N, Abramov AY. Mitochondria and lipid peroxidation in the mechanism of neurodegeneration: finding ways for prevention. *Med Res Rev*. 2021;41(2):770–784. doi:10.1002/med.21712
- Ayton S, Portbury S, Kalinowski P, et al. Regional brain iron associated with deterioration in Alzheimer's disease: a large cohort study and theoretical significance. *Alzheimers Dement*. 2021;17(7):1244–1256. doi:10.1002/alz.12282
- Zhou Q, Yang L, Li T, et al. Mechanisms and inhibitors of ferroptosis in psoriasis. *Front Mol Biosci*. 2022;9:1019447. doi:10.3389/fmolb.2022.1019447
- Vats K, Kruglov O, Mizes A, et al. Keratinocyte death by ferroptosis initiates skin inflammation after UVB exposure. *Redox Biol*. 2021;47:102143. doi:10.1016/j.redox.2021.102143
- Kajitani GS, Quayle C, Garcia CCM, et al. Photorepair of either CPD or 6-4PP DNA lesions in basal keratinocytes attenuates ultraviolet-induced skin effects in nucleotide excision repair deficient mice. *Front Immunol*. 2022;13:800606. doi:10.3389/fimmu.2022.800606
- Kim DJ, Iwasaki A, Chien AL, et al. UVB-mediated DNA damage induces matrix metalloproteinases to promote photoaging in an AhR- and SP1-dependent manner. *JCI Insight*. 2022;7(9):e156344. doi:10.1172/jci.insight.156344
- Bang E, Kim DH, Chung HY. Protease-activated receptor 2 induces ROS-mediated inflammation through Akt-mediated NF- κ B and FoxO6 modulation during skin photoaging. *Redox Biol*. 2021;44:102022. doi:10.1016/j.redox.2021.102022
- Gu Y, Han J, Jiang C, Zhang Y. Biomarkers, oxidative stress and autophagy in skin aging. *Ageing Res Rev*. 2020;59:101036. doi:10.1016/j.arr.2020.101036
- Dixon SJ, Lemberg KM, Lamprecht MR, et al. Ferroptosis: an iron-dependent form of nonapoptotic cell death. *Cell*. 2012;149(5):1060–1072. doi:10.1016/j.cell.2012.03.042
- Mishima E, Ito J, Wu Z, et al. A non-canonical vitamin K cycle is a potent ferroptosis suppressor. *Nature*. 2022;608(7924):778–783. doi:10.1038/s41586-022-05022-3

Clinical, Cosmetic and Investigational Dermatology

Dovepress

Publish your work in this journal

Clinical, Cosmetic and Investigational Dermatology is an international, peer-reviewed, open access, online journal that focuses on the latest clinical and experimental research in all aspects of skin disease and cosmetic interventions. This journal is indexed on CAS. The manuscript management system is completely online and includes a very quick and fair peer-review system, which is all easy to use. Visit <http://www.dovepress.com/testimonials.php> to read real quotes from published authors.

Submit your manuscript here: <https://www.dovepress.com/clinical-cosmetic-and-investigational-dermatology-journal>